JOC Article

Photophysical, Crystallographic, and Electrochemical Characterization of Symmetric and Unsymmetric Self-Assembled Conjugated Thiopheno Azomethines

Sergio Andrés Pérez Guarìn, Marie Bourgeaux, Stéphane Dufresne, and W. G. Skene*

Department of Chemistry, Pavillon JA Bombardier, University of Montreal, CP 6128, succ. Centreville, Montreal, Quebec H3C 3J7, Canada

w.skene@umontreal.ca

Received January 17, 2007

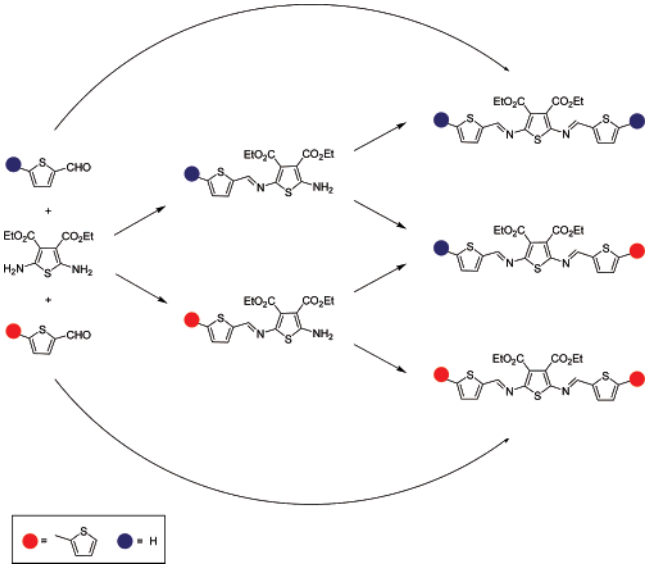

Novel conjugated azomethines consisting uniquely of thiophene units are presented. The highly conjugated compounds were synthesized by simple condensation of a stable diamino thiophene (**2**) with its complementary thiophene aldehydes. These interesting nitrogen-containing thiophene units exhibit variable reactivity leading to controlled aldehyde addition. Because of the different amino reactivity, a one-pot synthesis of unsymmetric and symmetric conjugated azomethines with varying number of thiophene units was possible by judicious choice of solvent and careful control of reagent stoichiometry. The resulting covalent conjugated connections are both reductively and hydrolytically resistant. The thermodynamically *E* isomer is formed uniquely for all of the azomethines synthesized, which is confirmed by crystallographic studies. These also demonstrated that the azomethine bonds and the thiophene units are highly planar and linear. The fluorescence and phosphorescence of the thiopheno azomethines measured are similar to those of thiophene analogues currently used in functional devices, but with the advantage of low triplet formation and band-gaps as low as 1.9 eV. The time-resolved and steady-state temperature-dependent photophysics revealed the thiopheno azomethines do not populate extensively their triplet manifold by intersystem crossing. Rather, their excited-state energy is dissipated predominantly by nonradiative means of internal conversion. Quasi-reversible electrochemical radical cation formation of the thiophene units was found. These compounds further undergo electrochemically induced oxidative cross-coupling, resulting in conjugated products that also exhibit reversible radical cation formation.

Introduction

Applications of conjugated materials such as organic light emitting diodes and molecular wires are highly sought after in technological applications due to their optical, emitting, and conducting properties.[1] Conjugated materials with these properties can be used in flexible light displays or low power consumption products,[2] including field effect transistors.[3] Because of these potential applications, great effort has focused on the synthesis of these and other new compounds with

10.1021/jo070100o CCC: $37.00
Published on Web 03/08/2007

CHART 1. Azomethines Examined and Some Representative Nitrogen-Free Derivatives

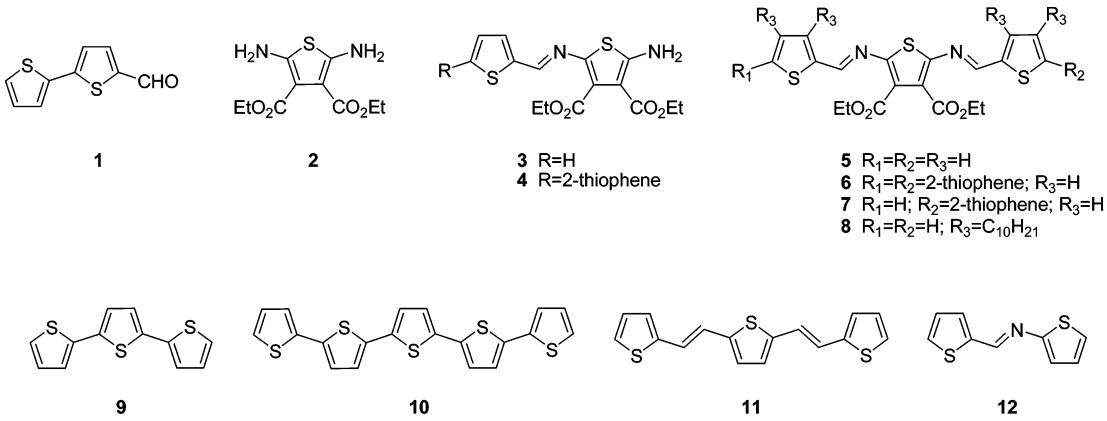

enhanced properties.[4] Even though research endeavors have concentrated on synthetic optimization, the synthesis of conjugated materials is unfortunately not a simple process.[5,6] Conventional synthetic methods require challenging and tedious purifications to isolate the desired conjugated materials.[6] Therefore, simple, high-yielding synthetic protocols for the preparation of unsymmetrical modules with tunable physical properties are quite rare.

Azomethines (−N═C−) are highly attractive alternatives to currently used conjugated materials. This is due in part to their isoelectronic character relative to their carbon analogues.[7] They are further advantageous because of their simple synthesis without the use of stringent reaction conditions or metal catalysts. They are easily purified, unlike their carbon analogues, and also exhibit high chemical and reductive resistance.[8,9] The limited number of stable diamino monomer precursors has unfortunately hindered the development of functional materials incorporating azomethines. Moreover, inadequate electrical/conductive properties, poor solubility, undesired oxidative decomposition, and irreversible radical cation formation are problematic with current azomethines and their diamino precursors, which further preclude their use as functional materials.[10] The 3,4-diethyl ester 2,5-diaminothiophene (**2**) is a propitious precursor for novel conjugated azomethines.[11] In addition to consisting of a thiophene moiety, which is highly desired because of its low oxidation potential, **2** also exhibits a high stability. This is in contrast to its unsubstituted analogue that cannot be isolated and spontaneously decomposes under ambient conditions. Because thiophenes have gained a wide importance due to their spectroscopic and electrochemical properties, azomethines derived from them would therefore possess ideal properties and be suitable for functional materials.[8,12,13]

The potential advantages of azomethine-based materials concomitant with our previous success with such compounds[14] have prompted us to develop simple synthetic routes to such materials containing only thiophene units. The main objective is to examine the physical properties, among which are the singlet and triplet states, and the fate of the excited states of these new compounds. These are of particular interest given the limited number of photophysical studies involving azomethines and their thiophene derivatives. The present report describes the synthesis and characterization of unprecedented thiopheno azomethines derived from **2** (Chart 1). Because of the different reactivities of the amino groups between **2** and the monoazomethine products, factors such as stoichiometry and judicious choice of solvent are examined for selective product formation. A one-pot modular synthesis of symmetric and unsymmetric self-assembled conjugated azomethines consisting of up to five thiophenes is investigated. The resulting photophysical, electrochemical, and band-gap properties, in addition to crystallographic data of these unique and highly conjugated thiopheno azomethines, are also presented.

Results and Discussion

Modular Synthesis. We originally sought out to synthesize **5** by a simple self-assembled approach using the stable diamino thiophene **2** because azomethines of this type have not yet been investigated. Additionally, we wanted to illustrate the stability

(1) (a) MacDiarmid, A. G. *Angew. Chem., Int. Ed.* **2001**, *40*, 2581−2590. (b) Dimitrakopoulos, C. D.; Malenfant, P. R. L. *Adv. Mater.* **2002**, *14*, 99−117. (c) Holliday, B. J.; Swager, T. M. *Chem. Commun.* **2005**, 23−36.

(2) (a) Rupprecht, L. *Conductive Polymers and Plastics in Industrial Applications*; Society of Plastics Engineers/Plastics Design Library: Brookfield, CT, 1999. (b) Brabec, C. J.; Sariciftci, N. S.; Hummelen, J. C. *Adv. Funct. Mater.* **2001**, *11*, 15−26.

(3) Katz, H. E.; Dodabalapur, A.; Bao, Z. In *Handbook of Oligo- and Polythiophenes*; Fichou, D., Ed.; Wiley-VCH Verlag GmbH: Weinheim, Germany, 1999; pp 459−489.

(4) Jenekhe, S. A. *Chem. Mater.* **2004**, *16*, 4381−4382.

(5) Lavastre, O.; llitchev, I. I.; Jegou, G.; Dixneuf, P. H. *J. Am. Chem. Soc.* **2002**, *124*, 5278−5279.

(6) (a) Kraft, A.; Grimsdale, A. C.; Holmes, A. B. *Angew. Chem., Int. Ed.* **1998**, *37*, 402−428. (b) Leclerc, M. *J. Polym. Sci., Part A: Polym. Chem.* **2001**, *17*, 2867−2873.

(7) (a) Wang, C.; Shieh, S.; LeGoff, E.; Kanatzidis, M. G. *Macromolecules* **1996**, *29*, 3147−3156. (b) Yang, C.-J.; Jenekhe, S. A. *Chem. Mater.* **1991**, *3*, 878−887.

(8) Thomas, O.; Inganäs, O.; Andersson, M. R. *Macromolecules* **1998**, *31*, 2676−2678.

(9) (a) Kucybala, Z.; Pyszka, I.; Marciniak, B.; Hug, G. L.; Paczkowski, J. *J. Chem. Soc., Perkin Trans. 2* **1999**, 2147−2154. (b) Skopalová, J.; Lemr, K.; Kotouèek, M.; Èáp, L.; Barták, P. *Fresenius' J. Anal. Chem.* **2001**, *370*, 963−969.

(10) (a) Suematsu, K.; Nakamura, K.; Takeda, J. *Colloid Polym. Sci.* **1983**, *261*, 493−501. (b) Morgan, P. W.; Kwolek, S. L.; Pletcher, T. C. *Macromolecules* **1987**, *20*, 729−739.

(11) Gewald, V. K.; Kleinert, M.; Thiele, B.; Hentschel, M. *J. Prakt. Chem.* **1972**, *314*, 303−314.

(12) (a) Tsai, F.-C.; Chang, C.-C.; Liu, C.-L.; Chen, W.-C.; Jenekhe, S. A. *Macromolecules* **2005**, *38*, 1958−1966. (b) Kiriy, N.; Bocharova, V.; Kiriy, A.; Stamm, M.; Krebs, F. C.; Adler, H.-J. *Chem. Mater.* **2004**, *16*, 4765−4771.

(13) Skene, W. G. WO 2005073265, 2005.

(14) (a) Skene, W. G.; Dufresne, S. *Org. Lett.* **2004**, *6*, 2949−2952. (b) Bourgeaux, M.; Pérez Guarìn, S. A.; Skene, W. G. *J. Mater. Chem.* **2007**, *17*, 972−979. (c) Dufresne, S.; Bourgeaux, M.; Skene, W. G. *J. Mater. Chem.* **2007**, 10.1039/b616379c. (d) Bourgeaux, M.; Skene, W. G. *Macromolecules* **2007**, *40*, 1792−1795.

SCHEME 1. General Synthetic Scheme Leading to Diamino Thiophene 2

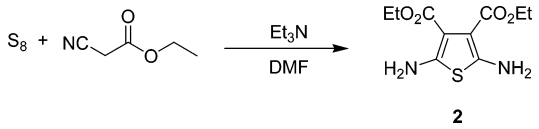

2

of **2** because of its electron-withdrawing ester groups and to demonstrate its usefulness as a precursor for new conjugated functional materials. It was anticipated that the physical properties of the resulting azomethine would mimic those of known carbon analogues such as **9** and **11**. The thiopheno azomethines were also anticipated to exhibit better properties than their homologous azomethines, making them useful for functional materials.

The key diamino thiophene (**2**) precursor required for the condensation with the thiophene aldehydes was synthesized according to a modified Gewald's reaction (Scheme 1).[11,26] This compound is particularly interesting because its electron-withdrawing esters reduce the amine's reactivity. The additional effect of the ester groups is the increased stability of **2** such that it can be obtained as a solid and can be handled without any special inert requirements. Conversely, its unsubstituted analogue cannot be isolated, and it spontaneously decomposes once exposed to ambient conditions. The deactivating esters also decrease the amine nucleophilicity, making its condensation with an aldehyde more difficult. Such is the reason for failed coupling reactions to afford any significant amount of the bisazomethines **5**−**7** under standard azeotrope distillation in anhydrous solvents such as toluene, THF, or with other typical mild dehydration methods. These mild conditions provide only the monoazomethines **3** or **4** regardless of the reaction conditions and the number of aldehyde equivalents used. Highly polar solvents such as DMF and high reaction temperatures are required to displace the equilibrium as to favor the second condensation and to afford the bisazomethines **5**−**8**. The azomethine bond of **3** and **4** has a strong electron-withdrawing character that exerts a combined effect with the ester withdrawing groups to further deactivate the primary amine. Stringent conditions are consequently required to activate the amine and to allow the second condensation to proceed for bisazomethine formation. Thus, a method for selective product formation is possible because of the inherent different amine reactivity, which can be exploited by using different solvents and stoichiometry.

TABLE 1. Product Distribution Obtained with Various Solvents and Aldehyde Stoichiometries

reagent ratio **1**/2TC[b]	solvent	% product distribution[a] **3**	**4**	**5**	**6**	**7**
2/2	ethanol	52	48			
1/1		52	48			
0.7/0.3		24	76			
0.3/0.7		73	27			
2/2	isopropanol	35	40	10	7	8
1/1		35	33	11	10	11
0.3/0.7		71	17	7	3	2
0.7/0.3		16	75	5	3	1
2/0			83		17	
0/2		79		21		
2/2	*n*-butanol	43	56	<1	<1	
1/1		52	48			
0.3/0.7		29	71			
0.7/0.3		68	32			
2/0			100			
0/2		100				
2/2	DMSO	49	51			
1/1		50	50			
0.3/0.7		22	78			
0.7/0.3		68	32			
2/2	neat[c]	19	20	20	21	20
1/1		30	35	15	17	3
2/0[d]			36		64	
0/2[d]		46		54		

[a] Amounts determined by HPLC after reacting at 70 °C for 24 h. [b] Number of equivalents of **1** and 2-thiophene carboxaldehyde (2TC) relative to **2**. [c] Reaction done in the absence of solvent and heating to 50 °C for 10 min with a catalytic amount of trifluoroacetic acid. [d] Bisazomethines are quantitatively formed upon heating the neat mixture for an additional 5 min at 60 °C.

Such a selective product formation was tested with various solvents and with different aldehyde stoichiometries. Alcohol solvents were preferred because of their ability to be made readily anhydrous and their high volatility allowing for easy product isolation, unlike DMF and DMSO. Moreover, such properties displace the equilibrium to favor azomethine formation. With ethanol, **3** and **4** were quantitatively formed by refluxing either with 1 equiv of the corresponding aldehyde with **2** or with an excess of aldehyde at room temperature. Only a small amount of the bisazomethine (<1%) was observed when refluxing for more than 1 week with an excess of the corresponding aldehyde. The monoazomethines were quantitatively obtained in high purity upon removal of the solvent when using 1 equiv of aldehyde. Interestingly, the resulting product crystallizes as large block-like crystals by simple removal of the solvent after the reaction is completed. The crystals obtained are of high quality and are suitable for X-ray analysis without additional recrystallization efforts. The simple crystallization of the compounds indicates the high degree of crystallinity of these thiophene azomethines.[25]

Unlike with ethanol, the double condensation to afford the bisazomethines **5** or **6** was possible with either isopropanol (IPA) or *n*-butanol (BuOH) along with 2 equiv of the corresponding aldehyde. The polarity differences and higher boiling points of these two solvents are sufficiently different from ethanol as to overcome the decreased amino reactivity of the monoazomethine. The double condensation to afford the bisazomethine is also possible in the absence of solvent. Pure bisazomethines were quantitatively obtained without purification by heating 2 equiv of the corresponding aldehyde at 50 °C for 15 min without any solvent.

(15) Becker, R. S.; Seixas de Melo, J.; Maçanita, A. L.; Elisei, F. *J. Phys. Chem.* **1996**, *100*, 18683−18695.
(16) Seixas de Melo, J.; Elisei, F.; Becker, R. S. *J. Chem. Phys.* **2002**, *117*, 4428−4435.
(17) Seixas de Melo, J.; Burrows, H. D.; Svensson, M.; Andersson, M. R.; Monkman, A. P. *J. Chem. Phys.* **2003**, *118*, 1550−1556.
(18) Seixas de Melo, J.; Silva, L. M.; Arnaut, L. G.; Becker, R. S. *J. Chem. Phys.* **1999**, *111*, 5427−5433.
(19) Seixas de Melo, J.; Elisei, F.; Gartner, C.; Aloisi, G. G.; Becker, R. S. *J. Phys. Chem. A* **2000**, *104*, 6907−6911.
(20) Scaiano, J. C. *CRC Handbook of Organic Photochemistry*; CRC Press: Boca Raton, FL, 1989.
(21) Carmichael, I.; Hug, G. L. *J. Phys. Chem. Ref. Data* **1986**, *15*, 1−250.
(22) (a) Andrews, L. J.; Deroulede, A.; Linschltz, H. *J. Phys. Chem.* **1978**, *82*, 2304−2309. (b) Murphy, R. S.; Moorlag, C. P.; Green, W. H.; Bohne, C. *J. Photochem. Photobiol., A* **1997**, *110*, 123−129.
(23) Connelly, N. G.; Geiger, W. E. *Chem. Rev.* **1996**, *96*, 877−910.
(24) Skene, W. G. *Polym. Prepr.* **2004**, *45*, 252−253.
(25) Skene, W. G.; Dufresne, S.; Trefz, T.; Simard, M. *Acta Crystallogr.* **2006**, *E62*, o2382−o2384.
(26) (a) Skene, W. G. PCT Int. Appl., 2005. (b) Bourgeaux, M.; Vomsheid, S.; Skene, W. G. *Synth. Commun.* **2007**, in press.

SCHEME 2. Modular Synthesis of Symmetric and Unsymmetric Conjugated Thiophene Compounds via Solvent and Stoichiometry Control in the Presence of Trifluoroacetic Acid Catalyst[a]

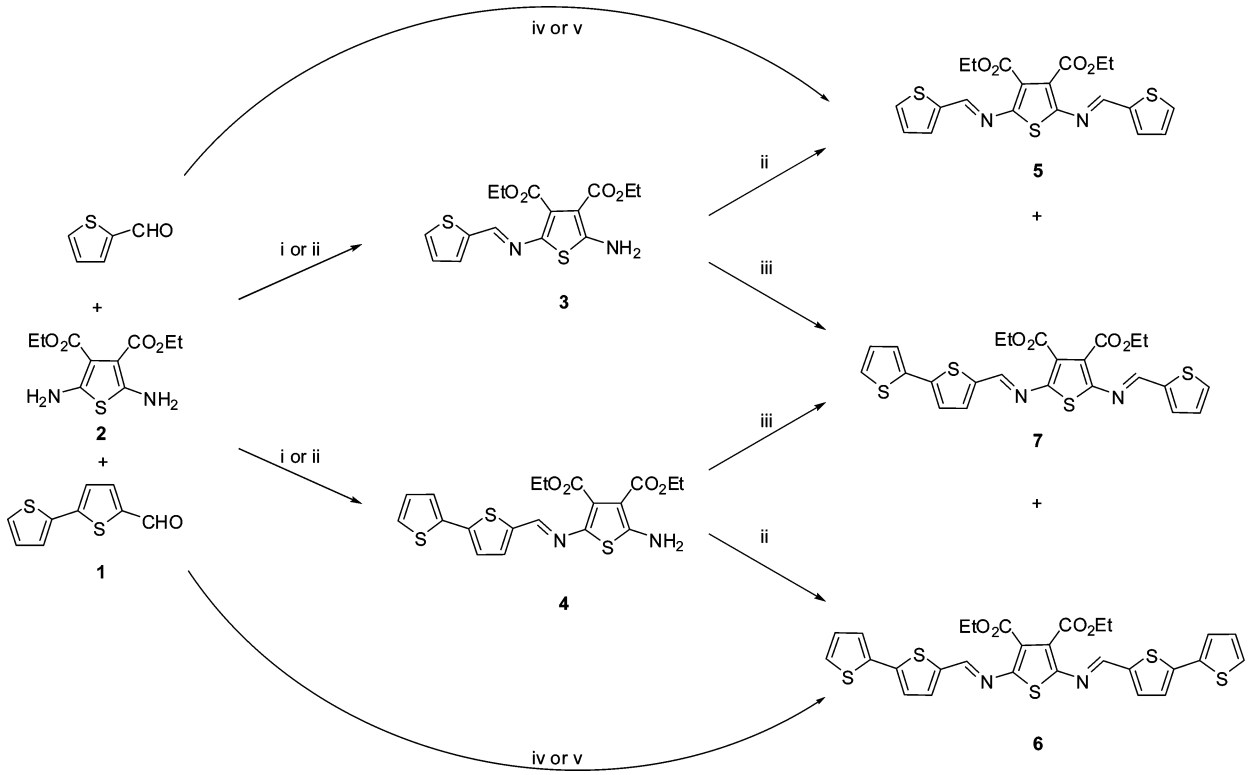

[a] (i) Refluxing ethanol with either 1 equiv or an excess of aldehyde, (ii) *n*-butanol or isopropanol with 1 equiv of aldehyde at 60 °C, (iii) *n*-butanol or isopropanol with 1 equiv of the corresponding aldehyde at 60 °C, (iv) *n*-butanol or isopropanol with 2 equiv of aldehyde at 60 °C, and (v) 2 equiv of aldehyde heating at 50 °C without solvent.

The reactivity differences of the amino group in the monoazomethine and that of **2** were further examined for selective product formation by judicious choice of solvent and reagent stoichiometry. The relative reactivities of **1** and 2-thiophene carboxaldehyde (2TC) toward **2** were first examined by reacting varying amounts of the aldehydes in different solvents and by examining the product distribution. A statistical product distribution consisting of monoazomethine, bisazomethine, and starting reagents is expected with 1 equiv of aldehyde in the absence of any product control. The resulting product distribution in Table 1 confirms that both aldehydes exhibit the same reactivity, because the product distribution parallels that of the aldehyde reagent ratios. The results further demonstrate that the condensation of **2** with an aldehyde forms quantitatively the monoazomethine before it undergoes the second condensation to afford to bisazomethine. Bisazomethine formation is only possible when IPA is used as the solvent. Formation of the bisazomethines was also possible with BuOH by further adding 1 equiv of aldehyde to the reaction medium followed by heating. The exclusive monoazomethine formation observed in the various solvents is a result of the amine reactivity differences between **2** and its corresponding monoazomethines. Such reactivity differences could be exploited to provide selective product formation in a stepwise/one-pot fashion by controlling parameters such as stoichiometry or solvent choice. Exclusive product formation of either the monoazomethines or the bisazomethines could ultimately be modulated via these parameters according to Scheme 2. To verify whether such a one-pot selective product formation was possible, we examined the use of different solvents in a sequential order along with various aldehyde amounts. The monoazomethine **3** was used as a benchmark because it could be quantitatively obtained from **2**[11,13,27] in ethanol with a stoichiometric amount of 2TC. Moreover, it has a characteristic ^{1}H NMR spectrum that lends itself to easy monitoring of the reaction progress via the large upfield shift of the imine proton as seen in Figure 1. Upon complete formation of **3** in ethanol, the solvent was removed whereupon the purity and its quantitative formation were verified by NMR. Isopropanol was then added along with 1 equiv of the corresponding aldehyde to afford either the symmetric (**5**) or the unsymmetric (**7**) bisazomethine upon heating. The same two-step/one-pot procedure also afforded **6** and **7** from **4** with the corresponding aldehydes. The symmetric bisazomethines were also formed from **2** with 2 equiv of aldehyde in isopropanol with heating. Because the corresponding monoazomethine is exclusively formed regardless of the solvent used, we exploited this for the one-pot synthesis of **7** in IPA. The use of 1 equiv of aldehyde in IPA afforded exclusively either the monoazomethine **3** or **4**, depending on the aldehyde selected. One equivalent of the other corresponding aldehyde was then added directly to the reaction mixture to afford the unsymmetric bisazomethine with heating. Therefore, selective formation of either symmetric or unsymmetric conjugated compounds ranging from 1 to 5 thiophene units can be had exclusively in a one-pot method according to Scheme 2.

All compounds were easily identified by their characteristic imine peak via ^{1}H NMR in the range of 8.2−8.8 ppm as seen in Figure 1. Interestingly, only one imine singlet was observed for all of the azomethines studied, implying the exclusive formation of one isomer. Only in the case of **7** were two imine

(27) Skene, W. G.; Trefz, T. *PMSE Prepr.* **2004**, *91*, 326−327.

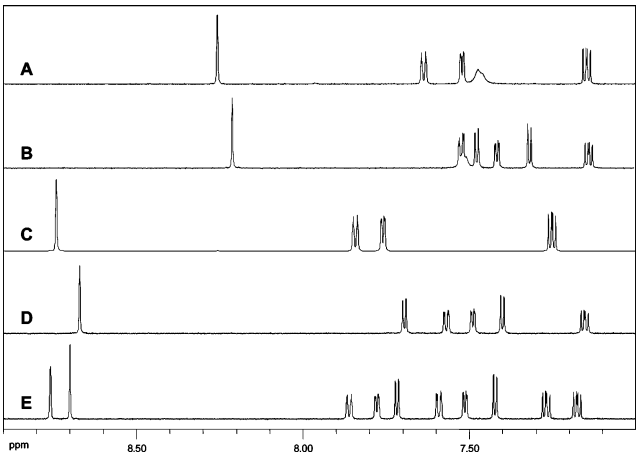

FIGURE 1. ^{1}H NMR spectra of thiopheno azomethines in deuterated acetone: A = **3**, B = **4**, C = **5**, D = **6**, and E = **7**.

peaks detected because it possesses two nonequivalent imines. Absolute assignment to either the *E* or the *Z* isomer for the products is, however, not possible by NMR and can only be had by X-ray crystal structure analysis (vide infra).

It is generally understood that azomethine formation is reversible, and, as a result, the products can be easily hydrolyzed. Because of the high degree of conjugation exhibited by **3**−**8** due to the azomethine bond, these compounds are expected to be relatively stable, and such is the case. This is supported by the lack of noticeable product decomposition under prolonged ambient humid conditions that would otherwise hydrolyze other azomethines. The azomethine stability is also evidenced by the lack of reaction with common reducing reagents such as $NaBH_3CN$, $NaBH_4$, high-pressure H_2/Pd, and even DIBAL, using standard protocols.[14] No apparent reduction of the azomethine bond was observed after refluxing in the presence of DIBAL for 16 h. Furthermore, the thiopheno azomethines have a high degree of resistance to oxidative decomposition unlike their carbon analogues.[28] The stability of the thiopheno azomethines is further evidenced through their resistance to photodecomposition and photoisomerization with intense laser irradiation at 355 nm. The condensation between **2** and aromatic aldehydes therefore leads to strong self-assembled bonds that can be considered as molecular "snaps". The bond can be snapped together with mild dehydration and can only be unsnapped with harsh conditions such as refluxing in concentrated sulfuric acid. Similarly to the azomethine robustness, **2** is also resistant, evidenced by the lack of observed acid-catalyzed transesterification of the thiopheno esters, which otherwise occurs with other esters under the experimental protocols employed.

Spectroscopic Properties. The absorption spectra show the degree of conjugation of the adducts, resulting from the azomethine bond, and they are comparable to their nitrogen-free derivatives. The linear trend observed for the reciprocal number of atoms along the conjugated framework versus the absorption shift shown in Figure 2 supports the conjugated nature of the azomethine bond. There is a resulting increase in stabilization with each additional thiophene ring, consistent with a planar and rigid π-conjugation. The absorption and emission spectra provide information relating to the energy differences between the excited and ground states for the thiophene

(28) Horowitz, G. *Adv. Mater.* **1998**, *10*, 365−377.

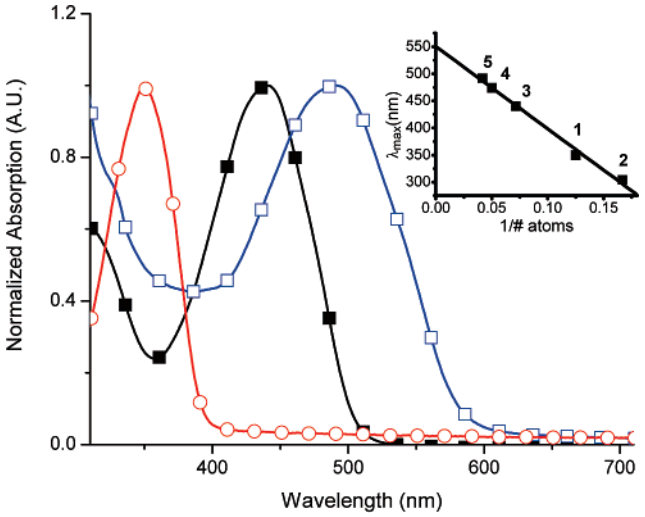

FIGURE 2. Normalized ground-state absorption spectra of **1** (○), **4** (■), and **7** (□) measured in anhydrous acetonitrile. Inset: Shift in absorbance maxima versus the number of atoms in the conjugated framework for compounds **1**−**5**.

azomethines.[29] The energy gap (ΔE) reported in Table 2 for the azomethines is lower than that for some representative analogues **9**−**11**. This is a result of the energy levels undergoing a pronounced stabilization from the heteroconjugated bond and the electron-withdrawing ester groups. The latter perturb the LUMO level, which affect the spectroscopic and electrochemical properties. The fluorescence spectra also show a bathochromic shift that correlates with the enhanced degree of conjugation because of the increased stabilization that occurs with increasing the number of thiophenes. The lack of structured emission observed in the fluorescence spectra suggests there is no defined order in the singlet excited and ground states and is consistent with other oligothiophenes.

Accurate band-gap energies can be obtained from the absorption onset because little difference between the absorbances in solution and in thin films was observed. Thin films are known to increase the planarity of twisted molecules, leading to increased conjugation concomitant with an absorption bathochromic shift. The absence of spectroscopic shift supports the crystallographic data (vide infra) that the thiopheno azomethines are linear and planar both in solution and in thin films. These structural effects contribute to the high delocalization and to the high degree of conjugation exhibited by the azomethines. This is further supported by the observed band-gap narrowing that occurs with increasing the number of thiophenes in the compounds examined. The resulting effect is band-gaps that are lower than those of their nitrogen-free derivatives, as seen in Table 2.

The excited-state properties of the unique thiopheno azomethines were determined by steady-state and time-resolved fluorescence. The measured fluorescence lifetimes are consistent with a unimolecular deactivation process. Because low fluorescence quantum yields were measured (Table 2) along with low radiative rate decay constants (k_f) for all of the compounds relative to bithiophene, the excited-state deactivation modes must occur by nonradiative channels such as internal conversion (IC) or intersystem crossing (ISC) to the triplet state. The latter results

(29) Van Der Looy, J. F. A.; Thys, G. J. H.; Dieltiens, P. E. M.; De Schrijver, D.; Van Alsenoy, C.; Geise, H. J. *Tetrahedron* **1997**, *53*, 15069−15084.

TABLE 2. Photophysical Data of Thiopheno Azomethines and Some Nitrogen-Free Derivatives Measured in Anhydrous Acetonitrile

compound	λ_{abs} (nm)[a]	ϵ_{max} (M^{-1} cm^{-1})	λ_{em} (nm)[b]	ΔE (eV)[c]	E_g (eV)[d]	Φ_{fl}[e] (10^{-2})	τ_{fl} (ns)[f]	k_r (10^{-6} s^{-1})[g]	k_{nr} (10^{-8} s^{-1})[h]	λ_{phos} (nm)[i]	τ_{ph} (ms)[j]	E_T (eV)[k]
1	350	21 850	425	3.2	3.1	2.3	0.9	26	11	441	4.5	2.8
2	305	9500	335	3.7		3.8	13.5	2.8	0.7	521	11.3	2.4
3	400	19 000	480	2.9	2.6	0.29	14.0	0.2	0.7	691	6.4	1.8
4	466	25 500	541	2.5	2.3	0.06	6.2	0.1	1.6	700	6.2	1.8
5	440	27 300	534	2.6	2.3	0.28	13.2	0.2	0.8	703	6.3	1.8
6	492	31 700	592	2.2	1.9	0.42	5.8	0.7	1.7	709	6.5	1.7
7	470	30 300	581	2.2	2.1	0.38	7.2	0.5	1.4	705	4.7	1.8
8	440	27 100	529	2.6	2.3	0.40	3.1	0.2	4.9	703	5.9	1.8
9[l]	351	24 200	405	3.1	3.2	9.0	0.2	450	46	653	0.06	1.9
10[l]	413	42 700	479	2.7	2.4	33	0.9	367	7.4	720	0.02	1.7
11[m]	423	30 000	445	2.5	2.8							

[a] Absorption. [b] Fluorescence. [c] Absolute HOMO−LUMO difference. [d] Spectroscopic band-gap. [e] Fluorescence quantum yield relative to bithiophene.[19] [f] Fluorescence lifetime. [g] Radiative rate constant $k_r = \phi_{fl}/\tau_f$. [h] Nonradiative rate constant $k_{nr} = k_r(1 - \phi_{fl})/\phi_{fl}$. [i] Phosphorescence maximum at 77 K in a 1:4 methanol/ethanol matrix. [j] Phosphorescence lifetimes measured at λ_{max}. [k] Triplet energy. [l] Literature values.[15,16,19,30] [m] Literature values.[56]

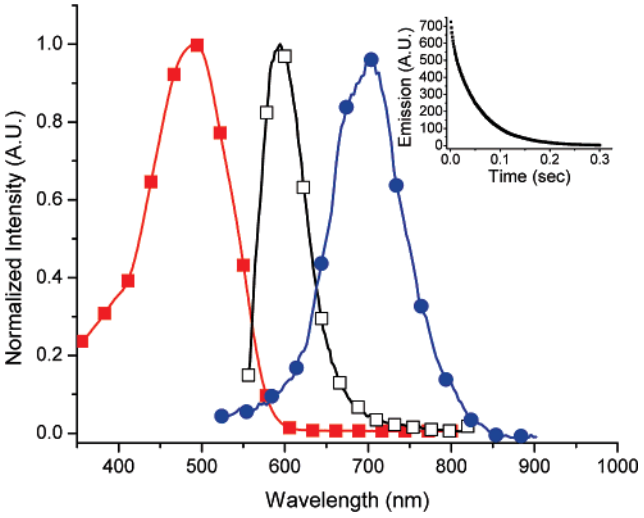

FIGURE 3. Spectroscopic properties of **6**. Normalized absorption (■) and fluorescence (□) recorded in deaerated acetonitrile, and phosphorescence (●) recorded at 77 K in a 1:4 methanol/ethanol glass matrix. The emission spectra were recorded with $\lambda_{ex} = 492$ nm. Inset: The phosphorescence lifetime measured at 700 nm with $\lambda_{ex} = 492$ nm.

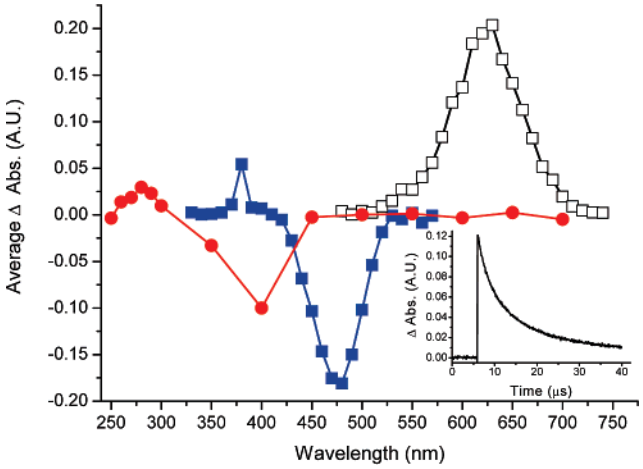

FIGURE 4. Transient absorption spectra of triplets measured in deaerated acetonitrile 100 μs after the laser pulse at 355 nm: xanthone (□), **3** (●), and **5** (■). The spectra were recorded under the exact conditions using optically matched samples at the laser excitation wavelength. Inset: Decay of xanthone triplet measured at 625 nm.

in efficient triplet manifold population that subsequently undergoes energy dissipation by either phosphorescence or nonradiative intersystem crossing. The singlet to triplet manifold shift is consistent with other thiophenes as a result of the sulfur atom that induces spin orbit coupling by the heavy atom effect.[15,17,18] The manifold shift was further expected to be enhanced by the azomethine nitrogen because it can potentially contribute to the heavy atom effect. The spin orbital coupling to populate the triplet manifold is supported by the phosphorescence measurements at 77 K, which show a bathochromic emission relative to the fluorescence emission (Figure 3). The phosphorescence quantum yields of ca. 0.1 can be measured for all of the thiopheno azomethines at this low temperature. Triplet energies can also be obtained by this spectroscopic method, which are comparable to those of terthiophene.[30,31] Additional evidence for the triplet nature is derived from its direct visualization by nanosecond-laser flash photolysis. Weakly absorbing transients are observed at 280 and 370 nm for the monoazomethine and the bisazomethine, respectively, by laser flash photolysis, shown in Figure 4. The bathochromic shift of the bisazomethine transient relative to the monoazomethine is consistent with its higher degree of conjugation. The extent of the week signal observed for the azomethine transients is evident when compared to the strongly absorbing xanthone triplet (Figure 4). The strong ground-state bleaching is also clearly seen in the transient absorption spectra of the azomethines and correlates well with ground-state absorption spectra. The negative bleaching signal corresponds to a strong ground-state absorption and hence a weak transient absorption at the wavelength studied. The observed transients are ascribed to the low-lying triplet because they are quenched by oxygen and they decay with first-order kinetics. Conversely, deactivation of a radical cation reactive intermediate would follow second-order kinetics involving bimolecular radical cation coupling. A unimolecular decay was also observed in the phosphorescence measurements that showed lifetimes on the order of milliseconds, similar to other low temperature reports.[15,17,30] These lifetimes are 2 orders of magnitude longer than conventional thiophenes at room temperature because of the lack of diffusion-controlled processes at 77 K. Faster phosphorescent lifetimes are therefore expected at room temperature, and these are further expected to be comparable to the lifetimes of other thiophenes.

Even though a triplet intermediate was detected by laser flash photolysis, it cannot be quantified because of its extremely weak

(30) Wasserberg, D.; Marsal, P.; Meskers, S. C. J.; Janssen, R. A. J.; Beljonne, D. *J. Phys. Chem. B* **2005**, *109*, 4410−4415.
(31) Wasserberg, D.; Dudek, S. P.; Meskers, S. C. J.; Janssen, R. A. J. *Chem. Phys. Lett.* **2005**, *411*, 273−277.

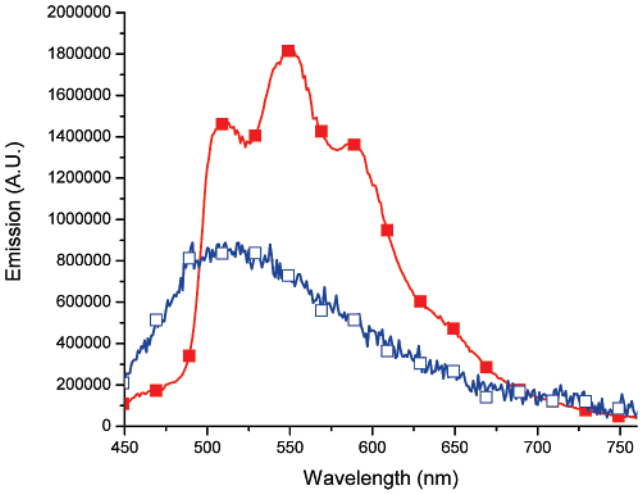

FIGURE 5. Fluorescence of **7** in a 1:4 methanol/ethanol mixture at 77 K (■) and room temperature (□; magnified 200 times).

signal. The weak signal for the triplet thiopheno azomethines is unexpected because these compounds are highly conjugated and should therefore exhibit strong triplet extinction coefficients (ϵ_T), such as $\epsilon_T = 13\,000\ M^{-1}\ cm^{-1}$ for bithiophene, for example.[17,32] Both the quantum yield of triplet formation and the ϵ_T contribute to the signal intensity in laser flash photolysis. Because of their high degree of conjugation, the thiopheno azomethines should possess a large ϵ_T. Therefore, the observed weak signal can occur only from a low yield of triplet formation. The yield can be calculated by measuring the change in transient signal of the azomethine (ΔAbs) with laser power versus that of xanthone, according to eq 1. Assuming a triplet extinction coefficient similar to that of bithiophene, an upper limit of 5% for the triplet quantum yield is calculated by this method. Even though the low value is in agreement with the phosphorescence quantum yields, it is surprising because thiophenes are known to have high triplet quantum yields, ~0.9.[15] To validate our results, we measured the Φ_T for bithiophene by the widely accepted method of relative actinometry with 1-methylnaphthalene.[20,33] Our measured value of 0.30 is in agreement with other studies[34] and differs from the previously measured values by photoacoustic calorimetry.[18] The discrepancy between these values can be in part due to the photoacoustic method, whose accuracy relies heavily on triplet lifetime being shorter than the detector's response time. This not withstanding, the low yield of triplet formation implies the major pathway for deactivation of the thiopheno azomethines occurs by internal conversion according to the following energy conversation equation: $\Phi_{fl} + \Phi_{ISC} + \Phi_{IC} \approx 1$. Therefore, the contribution from nonradiative emission by internal conversion for the thiopheno azomethines must be higher than that for oligothiophenes. Evidence for the IC deactivation mode is derived from the relative fluorescence at 77 K that is 260 times greater than that at room temperature (Figure 5). All modes of excited-state deactivation involving bond rotation are suppressed at this low temperature, leading to a dramatic fluorescence quantum yield increase. Because the fluorescence quantum yields at 77 K are determined by comparing the extremely weak fluorescence signal at room temperature relative to the intense signal at 77 K under the same experimental conditions, precise calculations of Φ_{fl} are difficult. This notwithstanding, an estimate of the low-temperature fluorescence quantum yield ~0.80 for all of the azomethines was found. Even though the predominant deactivation mode is by IC, approximately 20% of energy dissipation is unaccounted for and must therefore occur by ISC to the triplet. Nonradiative energy dissipation by *E*/*Z* photoisomerization of the azomethine bond is an alternate deactivation mode.[35] No photoisomers were, however, found for any of the compounds after irradiation for 12 h at 350 nm. Given the lack of significant signal by laser flash photolysis that would otherwise be highly visible, the imine bond must therefore be a good triplet deactivator leading to rapid and efficient intramolecular quenching of this excited state. Such is the case for acylhydrazides, which contain an imine-type linkage.[36]

$$\phi_{azomethine} = \frac{\epsilon_{azomethine}}{\epsilon_{xanthone}} \cdot \frac{\Delta Abs_{xanthone}}{\Delta Abs_{azomethine}} \cdot \phi_{xanthone}$$

Equation 1 was used to determine the azomethine triplet quantum yield ($\phi_{azomethine}$) relative to the triplet quantum yield of xanthone ($\phi_{xanthone}$), the triplet extinction coefficients (ϵ), and the change in maximum signal intensity with laser power (ΔAbs).

The energy levels, and hence the band-gap and the absorption properties, can be further modified by acid doping to give conductive-like properties to the azomethines. Methanesulfonic acid is a suitable p-dopant that protonates the azomethine and extends the degree of conjugation. A ca. 100 nm bathochromic shift for **5**−**7** occurs upon acid protonation. The increased stabilization from the nitrogen protonation results in a localized charge on the nitrogen. The remarkable visible color change denotes an increased delocalization and an additional band-gap stabilization of approximately 0.4 eV. Successive acid addition results uniquely in the protonated species given the presence of one isobestic point as seen in Figure 6. The addition of triethylamine neutralizes the cationic species and regenerates the neutral bisazomethine. Cycling between the protonated and the neutral forms via the successive addition of acid and base results in reversible color change with little degradation of the sample. Resistance to repetitive acid/base protonation/deprotonation further supports the persistence nature of the conjugated azomethine bond.

Cyclic Voltammetry. Thiophenes are readily oxidized by two stepwise one-electron oxidative processes, which can be observed in cyclic voltammetry. The first oxidation generates a radical cation that can cross-couple, provided unsubstituted α-positions are available. Continuous oxidization subsequently affords higher ordered oligomers by a radical-like coupling mechanism and ultimately the formation of polymers by successive oxidation. At higher potentials, a second oxidation affording the dication is possible. The thiopheno azomethines

(32) Wintgens, V.; Valat, P.; Garnier, F. *J. Chem. Phys.* **1994**, *98*, 228−232.
(33) Scaiano, J. C.; Lissi, E. A.; Stewart, L. C. *J. Am. Chem. Soc.* **1984**, *106*, 1539−1542.
(34) (a) Scaiano, J. C.; Redmond, R. W.; Mehta, B.; Arnason, J. T. *Photochem. Photobiol.* **1990**, *52*, 655−659. (b) Reyftmann, J. P.; Kagan, J.; Santus, R.; Morliere, P. *Photochem. Photobiol.* **1985**, *41*, 1−7.
(35) (a) Amati, M.; Bonini, C.; D'Auria, M.; Funicello, M.; Lelj, F.; Racioppi, R. *J. Org. Chem.* **2006**, *71*, 7165−7179. (b) Lehn, J.-M. *Chem.-Eur. J.* **2006**, *12*, 5910−5915.
(36) (a) Lygaitis, R.; Grazulevicius, J.; Van, F. T.; Chevrot, C.; Jankauskas, V.; Jankunaite, D. *J. Photochem. Photobiol., A* **2006**, *181*, 67−72. (b) Getautisa, V.; Grazulevicius, J. V.; Daskeviciene, M.; Malinauskas, T.; Gaidelis, V.; Jankauskas, V.; Tokarski, Z. *J. Photochem. Photobiol., A* **2006**, *180*, 23−27.

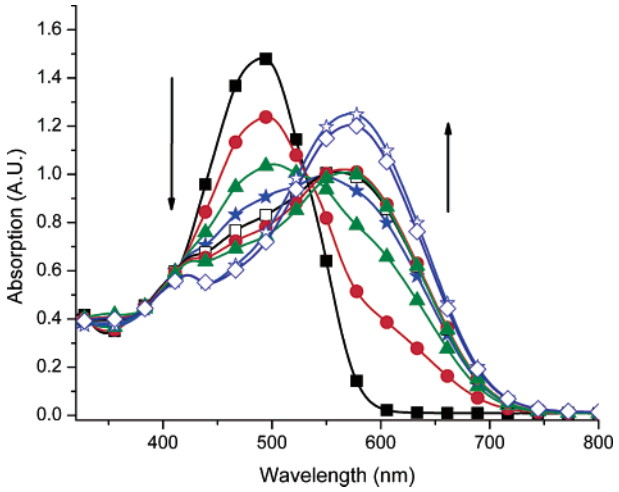

FIGURE 6. Absorption spectra change of **6** upon protonation with methanesulfonic acid in anhydrous acetonitrile. Mole percentage of acid added: 0 (■), 20 (●), 40 (▲), 60 (★), 80 (□), 100 (○), 120 (△), 140 (☆), 160 (◇).

TABLE 3. Electrochemical Data of Thiopheno Azomethines, Their Polymers, and Nitrogen-Free Derivatives[a]

compound	E_{pa}^1 (V)	E_{pa}^2 (V)	ΔE_{pa} (V)
1	1.02	1.24	0.22
2	0.04	0.4	0.36
3	0.91	1.37	0.46
4	0.83	1.07	0.24
5	1.16 (0.91)[b]	1.53	0.37
6	1.02 (1.06)[b]	1.37	0.35
7	0.99 (1.17)[b]	1.25	0.26
8	1.17 (1.05)[b]	1.51	0.34
9[e]	0.95	1.9	0.95
10[f]	0.82	1.12	0.30
11[c]	0.88 (0.95)[b,c]	1.14	0.26
12[c]	1.60 (2.09)[b,d]	1.88	0.28

[a] First and second oxidation potentials corresponding to the radical cation and the dication, respectively. In anhydrous and deaerated dichloromethane with Bu_4NPF_6 as the supporting electrolyte. Values are reported against SCE with ferrocene (0.59 V) as an internal standard.[23] [b] Values in parentheses refer to the oxidation potentials of oxidatively coupled materials deposited on the ITO electrode. [c] Literature values.[43] [d] Literature values.[37] [e] Literature values.[57] [f] Literature values.[58]

studied are of no exception. Two consecutive one-electron oxidations corresponding to the radical cation followed by the dication were observed for **5**−**8** (Table 3). Additionally, **2**−**4** undergo two one-electron oxidations of the amine group. For all of the azomethines studied, it is noteworthy that the first oxidation forms a quasi-reversible radical cation as seen in Figure 7A. This is in stark contrast to other azomethines such as **12** that undergo irreversible oxidation regardless of the experimental conditions because of their extreme reactivity. This behavior ultimately limits their usefulness as functional materials.[8,37−39] In fact, previous azomethine examples are so

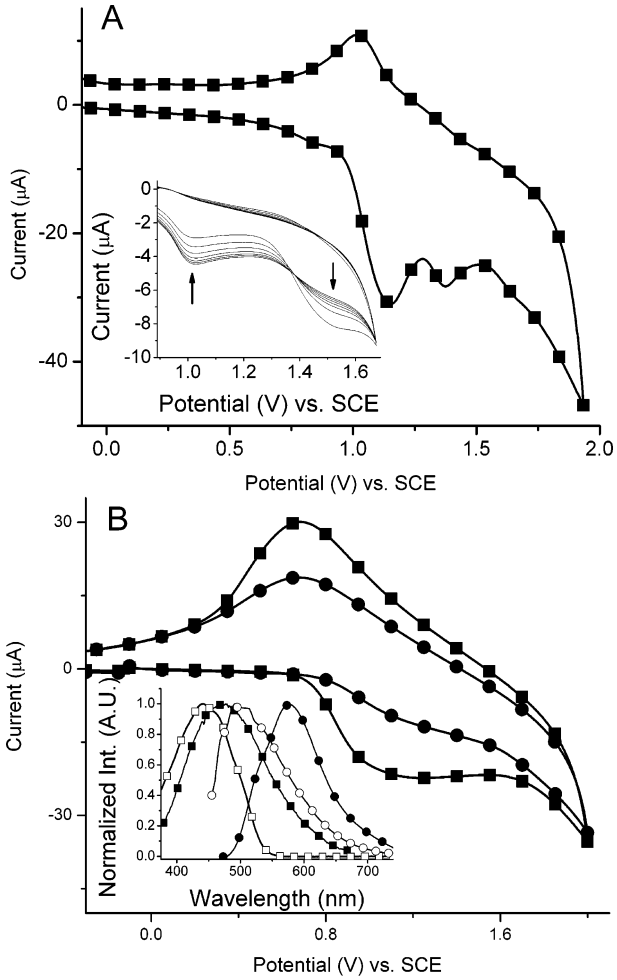

FIGURE 7. (A) Typical cyclic voltammogram of **6** recorded in anhydrous dichloromethane with Bu_4NPF_6 supporting electrolyte against Ag/AgCl electrode at 100 mV/s and referenced against SCE. Inset: Repeated cyclic oxidation of **6** between 0 and 1400 mV with the product deposited on the Pt working electrode. (B) Cyclic voltammogram of **P5** (●) and **P8** (■) deposited on ITO electrode after continued oxidative cross-coupling of **5** and **8**, respectively, recorded in deaerated dichloromethane under the same conditions as in (A). Inset: Normalized spectra of **8** (open symbols) in deaerated acetonitrile and **P8** (closed symbols) on ITO electrode; absorption (squares) and emission (circles). The emission spectra were recorded with $\lambda_{ex} = 400$ nm.

reactive they undergo both monomer and polymer oxidative decomposition. The persistent thiopheno azomethine radical cations imply a high degree of stability of the reactive intermediate, unlike other azomethine radical cations.

Because previous azomethine electrochemical studies involved only homologous aryl units they not only exhibited irreversible oxidation,[37,39,40] they also exhibited extremely high oxidation potentials. The thiophene-containing azomethines are advantageous because they possess lower oxidation potentials and they are comparable to other thiophenes. This is due in part to the two ester withdrawing groups, while the strong donating capacity of the amine group influences the oxidation potentials. This is obvious for **3** and **4** whose oxidation potentials are similar to those of the bisazomethines even though the latter have a higher degree of conjugation. The low oxidation

(37) Diaz, F. R.; del Valle, M. A.; Brovelli, F.; Tagle, L. H.; Bernede, J. C. *J. Appl. Polym. Sci.* **2003**, *89*, 1614−1621.
(38) (a) Yang, C.-J.; Jenekhe, S. A. *Macromolecules* **1995**, *28*, 1180−1196. (b) Lund, H.; Hammerich, O. *Organic Electrochemistry*, 4th ed.; Marcel Dekker: New York, 2001. (c) Caballero, A.; Tárraga, A.; Velasco, M. D.; Molina, P. *Dalton Trans.* **2006**, 1390−1398. (d) Catanescu, O.; Grigoras, M.; Colotin, G.; Dobreanu, A.; Hurduc, N.; Simionescu, C. I. *Eur. Polym. J.* **2001**, *37*, 2213−2216. (e) Grigoras, M.; Catanescu, C. O.; Colotin, G. *Macromol. Chem. Phys.* **2001**, *202*, 2262−2266.
(39) Higuchi, M.; Yamamoto, K. *Polym. Adv. Technol.* **2002**, *13*, 765−770.
(40) (a) Zotti, G.; Randi, A.; Destri, S.; Porzio, W.; Schiavon, G. *Chem. Mater.* **2002**, *14*, 4550−4557. (b) Brovelli, F.; Rivas, B. L.; Bernede, J. C. *J. Chilean Chem. Soc.* **2005**, *50*, 597−602.

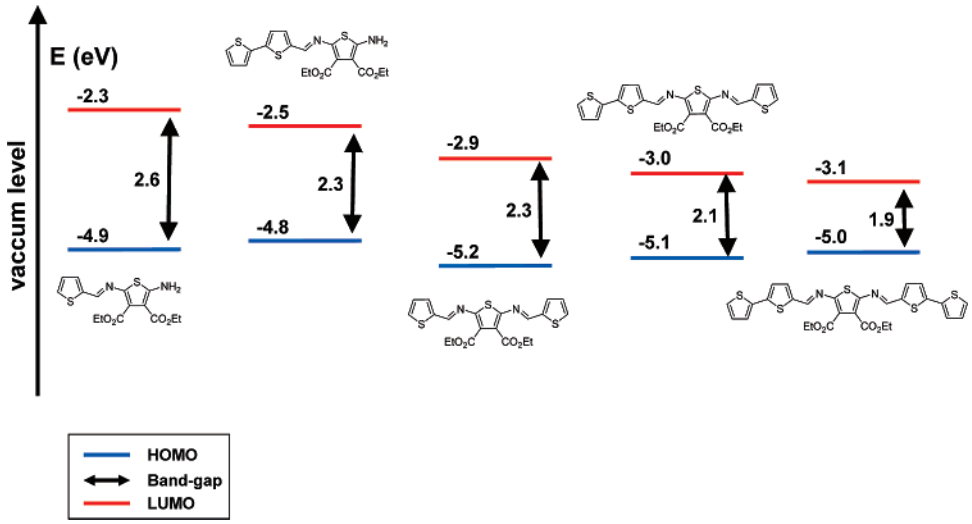

FIGURE 8. Schematic representation of the relative band-gaps and energy levels influenced by the number of thiophene groups.

potentials observed for the monoazomethines are a result of the stabilizing influence of the amino donating group, which decreases the HOMO energy level. The combined influence of the amino donating ability concomitant with the high degree of conjugation of the azomethines cause a significant lowering of the oxidation potentials. The monoazomethine oxidation potentials are highly perturbed by the amino group such that they are lower than their thiophene and bithiophene analogues, whose oxidation potentials are 2.07 and 1.05 V, respectively.[41]

The ionization potential (IP), corresponding to the HOMO energy level, can be calculated from the oxidation onset according to IP = E^{ox}_{onset}(SCE) + 4.4. The E_{onset} (SCE) is the oxidation potential onset in volts versus the SCE electrode to which a 0.39 V correction factor is applied. Similarly, the electron affinity (EA), corresponding to the LUMO energy level, can normally be calculated from the reduction onset (E^{red}_{onset}) according to EA = E^{red}_{onset}(SCE) + 4.4. Because of the lack of observed reduction under our experimental conditions, which further supports the azomethine robustness, the electron affinity can be calculated alternatively from the spectroscopic band-gap and from the ionization potential according to EA = IP − E_g. These data provide an accurate representation of the HOMO−LUMO energy levels and the band-gaps, which are schematically depicted in Figure 8. The stabilizing effect of the amino donating group on the HOMO is apparent in this figure. Furthermore, the effect of the number of thiophene groups and the conjugation degree upon reducing the band-gap is also apparent. The spectroscopic band-gaps demonstrate that values as low as 1.9 eV are possible with the thiopheno azomethines. This is different from their analogues whose band-gap lower limit is considerably higher at 2.4 eV.

Electrochemical Oxidative Coupling. Even though the thiopheno azomethine radical cation formation is quasi-reversible, it is, however, sufficiently reactive to undergo electrochemically induced oxidative cross-coupling (EIC). EIC of **5**−**8** was possible either by repetitive oxidative cycling between 0 and 1400 mV or by applying a potential greater than the corresponding radical cation for a period of 10 min. The resulting products were deposited as dark colored films on the working electrode.[42,43] The oxidative coupling results in an increase in the oxidation peak of the deposited material on the electrode concomitant with a decrease of the first oxidation peak of the monomer (inset Figure 7A). The increase in anodic peak potential for the deposited film relative to the monomer is attributed to the nonconductiveness of the deposited layer as a result of the ion diffusion rate determining step. This is well established for the electropolymerization of semiconductors and is consistent with other thiophenes.[44] The amount of product deposited is the same for **5**−**8** and corresponds to a charge of ca. 10^{-3} coulombs obtained by washing the resulting layer with copious amounts of acetonitrile and dichloromethane followed by measuring the redox potential of the insoluble product in monomer-free electrolyte.[45] The resulting redox properties of the cross-coupled products are reported in Table 3.

Because of previous studies that showed the radical cation azomethine intermediates are particularly reactive, their electrochemically induced oxidative coupling was expected to result in limited extension of their conjugation because of α−β and β−β coupling defects.[46] The EIC of **8** was investigated because its β positions do not allow for such defects and it would promote exclusively conjugated products via α−α coupling. The bathochromic shifts found for both the fluorescence and the absorption spectra (inset Figure 7B) suggest a product with a greater degree of conjugation relative to the monomer is formed. This can only occur by α−α coupling. Product coupling was further confirmed by large-scale electrochemical oxidative cross-coupling of **5** in which sufficient material was obtained for conventional molecular weight characterization by GPC. The

(41) Diaz, A. F.; Martinez, A.; Kanazawa, K. K.; Salmon, M. *J. Electroanal. Chem. Interfacial Electrochem.* **1981**, *130*, 181−187.

(42) (a) Hansford, K. A.; Guarin, S. A. P.; Skene, W. G.; Lubell, W. D. *J. Org. Chem.* **2005**, *70*, 7996−8000. (b) Haare, J. A. E. H. v.; Havinga, E. E.; Dongen, J. L. J. v.; Janssen, R. A. J.; Cornil, J.; Brédas, J.-L. *Chem.-Eur. J.* **1998**, *4*, 1509−1522.

(43) (a) Jérôme, C.; Maertens, C.; Mertens, M.; Jérôme, R.; Quattrocchi, C.; Lazzaroni, R.; Brédas, J. L. *Synth. Met.* **1996**, *83*, 103−109. (b) Jérôme, C.; Maertens, C.; Mertens, M.; Jérôme, R.; Quattrocchi, C.; Lazzaroni, R.; Brédas, J. L. *Synth. Met.* **1997**, *84*, 163−164.

(44) (a) Sun, X. B.; Liu, Y. Q.; Chen, S. Y.; Qiu, W. F.; Yu, G.; Ma, Y. Q.; Qi, T.; Zhang, H. J.; Xu, X. J.; Zhu, D. B. *Adv. Funct. Mater.* **2006**, *16*, 917−925. (b) Yassar, A.; Roncali, J.; Garnier, F. *Macromolecules* **1989**, *22*, 804−809. (c) Henderson, P. T.; Collard, D. M. *Chem. Mater.* **1996**, *7*, 1879−1889.

(45) Tourillon, G. In *Handbook of Conducting Polymers*; Skotheim, T. A., Ed.; Marcel Dekker, Inc.: New York, 1986; Vol. 1, pp 293−350.

(46) Roncali, J. *Chem. Rev.* **1992**, *92*, 711−738.

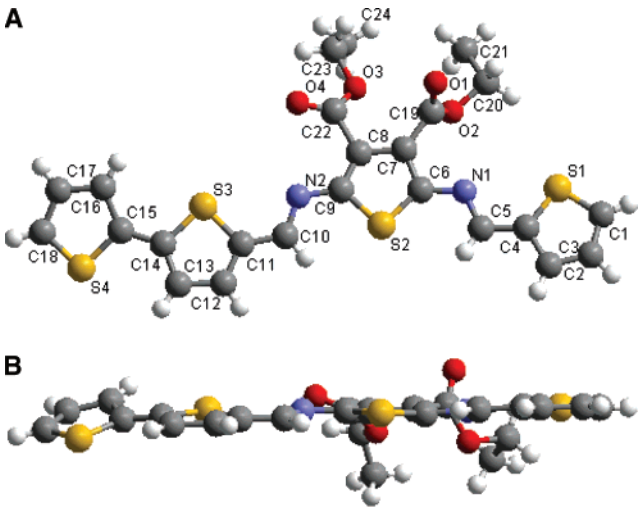

FIGURE 9. (A) Schematic representation of the crystal structure **7** showing the atomic labels. (B) Schematic representation of crystal structure **7** seen along the axis parallel to the thiophene units.

average molecular weight calculated corresponds to a product with 9 thiophene units. This represents a lower limit for the molecular weight of the coupled products and implies that the molecular weight of the bulk insoluble material is likely much higher. Further evidence for the increased conjugation of the coupled product is derived from the spectroscopic band-gap of the electrochemically produced product that is 0.5 eV lower than the corresponding monomer. Furthermore, both the absorption and the fluorescence spectra undergo pronounced bathochromic shifts relative to the monomer (inset Figure 7B) because of increased conjugation. The similarity between the spectroscopic and the redox properties of the products derived from **5** and **8** confirms the coupling occurs exclusively via the α position and results in an increased degree of conjugation. This is further supported by the broad reversible oxidation potentials that are indicative of a distribution of oxidation states associated with oligomers and polymers. The resulting coupled products exhibit oxidations similar to those of their nitrogen-free derivatives, and they can be reversibly oxidized at low potentials such that the azomethines can be p-doped with standard chemical dopants. This is in stark contrast to other conjugated azomethines that undergo complete irreversible radical cation formation regardless of the experimental conditions and scan rates. This irreversible behavior has limited the usefulness of other azomethines as functional materials.[37] The low oxidation potential concomitant with the reversible radical cation formation illustrate the suitability of thiophene azomethines as functional p-dopable materials.

X-ray Crystallography. Like their carbon analogues, two geometry isomers (*E* and *Z*) are possible with azomethines. Because the azomethine has only one proton that does not couple, both *E* and *Z* isomers are expected to provide only a singlet in ^{1}H NMR in the region of 8.5 ppm (Figure 1). Differentiation between these two is not readily possible by 1D and 2D NMR unlike their carbon analogues. Absolute assignment of the azomethine to the *E* isomer can, however, be derived from the crystallographic data (Figure 9). Formation of the thermodynamically stable *E* isomer is assumed for all of the azomethines given the presence of only one imine peak in all of the ^{1}H NMR spectra. This was confirmed by repeated crystallizations of **4**, **5**, and **7**, which consistently gave the same crystal structure and the *E* isomer. The crystals used for X-ray analyses were subsequently dissolved in deuterated acetone. The resulting NMR spectra showed an imine chemical shift identical to that of the original reaction mixture, confirming that the *E* isomer is uniquely formed.

TABLE 4. Representative Bond Distances and Mean Plane Angle for 7 and Its Nitrogen-Free Analogue

	7		**11**[a]	
	monothiophene[b]	bithiophene[c]	side A[d]	side B[d]
plane angle[g]	180°	170.1°	177.9°	180°
−X═X−[e]	1.343 Å	1.306 Å	1.300 Å	1.326 Å
−X−aryl[e]	1.387 Å	1.372 Å	1.460 Å	1.440 Å
═CH−aryl	1.423 Å	1.413 Å	1.452 Å	1.453 Å
sulfur orientation[g]	antiparallel	antiparallel	parallel	antiparallel

[a] From Zobel.[51] [b] Refers to distances and angles from S_1 through S_2 in Figure 9A. [c] Refers to distances and angles from S_2 through S_4 in Figure 9A. [d] Refers to each side of the unsymmetric molecule. [e] X = N for **7** and C for **11**. [f] Refers to angles between the central and the terminal thiophene mean planes. [f] Sulfur orientation relative to the central thiophene.

In addition to absolute assignment of the geometric isomer, the isolated crystal structure illustrated in Figure 9 shows the heteroatom units are orientated in an antiparallel arrangement. This is predominantly a result of the intramolecular hydrogen bonding of the donor−acceptor pairs between the central sulfur (S_2) and the imine hydrogens (H_5 and H_{10}). The antiparallel orientation is similar to that of bithiophene and other higher ordered oligothiophenes. Moreover, the planar configuration between the thiophene units and the azomethine is visible, in which the mean planes of the terminal thiophenes are twisted 2.6° and 8.0° from the azomethine plane (Table 4). This represents among the first few examples of reduced twisting of the azomethine mean planes.[25] This is in contrast to homoaryl aromatic rings that are normally twisted between 45° and 65° from the mean planes of azomethines to which they are directly bound.[14,47,48] This arrangement prevents any steric hindrance between the imine hydrogen and that of the aryl ortho hydrogen,[14,47] which would lead to an orthogonal biphenyl-type conformation.[49] The observed planarity disruption for such compounds limits their conjugation[50] and subsequently limits their usefulness as functional materials. The crystallographic data show the azomethine bond distances are shorter than those of its nitrogen-free derivative,[51,52] while the aryl−aryl distance remains unchanged.[53] The enhanced planarity observed for the studied azomethines is further responsible for the increased conjugation and ensuing narrow band-gaps and potentially results in ideal conductive when doped.[14,54] The high degree of planarity and linearity further results in an extremely tight

(47) Skene, W. G.; Dufresne, S. *Acta Crystallogr.* **2006**, *E62*, o1116−o1117.
(48) (a) Kuder, J. E.; Gibson, H. W.; Wychick, D. *J. Org. Chem.* **1975**, *40*, 875−879. (b) Manecke, G.; Wille, W. E.; Kossmehl, G. *Makromol. Chem.* **1972**, *160*, 111−126. (c) Bürgi, H. B.; Dunitz, J. D. *Chem. Commun.* **1969**, 472−473.
(49) Narasegowda, R. S.; Yathirajana, H. S.; Bolteb, M. *Acta Crystallogr., Sect. E* **2005**, *E61*, o939−o940.
(50) (a) Wan, C.-W.; Burghart, A.; Chen, J.; Bergström, F.; Johansson, L. B.-Å.; Wolford, M. F.; Kim, T. G.; Topp, M. R.; Hochstrasser, R. M.; Burgess, K. *Chem.-Eur. J.* **2003**, *9*, 4430−4441. (b) Jiao, G.-S.; Thoresen, L. H.; Burgess, K. *J. Am. Chem. Soc.* **2003**, *125*, 14668−14669.
(51) (a) Ruban, G.; Zobel, D. *Acta Crystallogr., Sect. B* **1975**, *B31*, 2632−2634. (b) Zobel, D.; Ruban, G. *Acta Crystallogr., Sect. B* **1978**, *B34*, 1652−1657.
(52) Blanchard, P.; Brisset, H.; Illien, B.; Riou, A.; Roncali, J. *J. Org. Chem.* **1997**, *62*, 2401−2408.
(53) Pelletier, M.; Brisse, F.; Cloutier, R.; Leclerc, M. *Acta Crystallogr., Sect. C* **1995**, *C51*, 1394−1397.
(54) Roncali, J.; Thobie-Gautier, C. *Adv. Mater.* **1994**, *6*, 846−848.

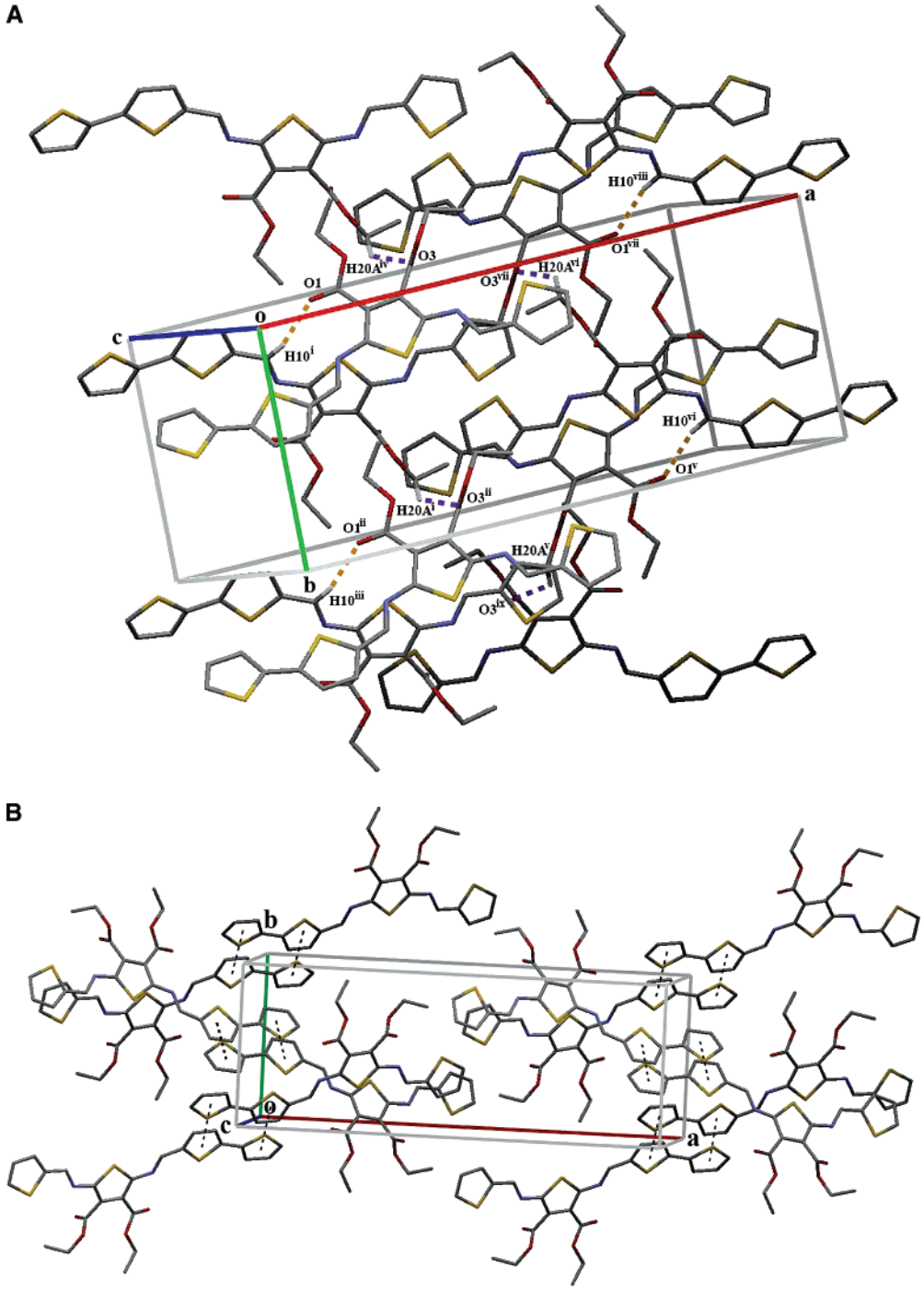

FIGURE 10. (A) Crystal packing arrangement of **7** illustrating the intermolecular hydrogen bonding between donor and acceptor pairs $O_1\cdots H_{10}$ and $O_3\cdots H_{20}$ (i (x, $^1/_2 - y$, $^1/_2 + z$); ii (x, $1 + y$, z); iii (x, $^3/_2 - y$, $^1/_2 + z$); iv (x, $-^1/_2 - y$, $^1/_2 + z$); v ($1 - x$, $1 - y$, $1 - z$); vi ($1 - x$, $^1/_2 + y$, $^1/_2 - z$); vii ($1 - x$, $-y$, $1 - z$); viii ($1 - x$, $-^1/_2 + y$, $^1/_2 - z$); ix ($1 - x$, $^3/_2 + y$, $^3/_2 - y$)). (B) Crystal packing arrangement of **7** illustrating the π-stacking interactions between adjacent bithiophenes.

packing arrangement in the crystal structure that is further enhanced by intermolecular hydrogen bonding between $O_1\cdots H_{10}$ (Figure 10A) and $O_3\cdots H_{20}$, π-stacking (Figure 10B) between S_3 and S_4 with their corresponding sulfurs in adjacent molecules, and C−H−π interactions between H_{16} and H_{17} with the π-system of S_3 and S_4. The resulting combined strong interactions result in a three-dimensional herringbone-like network.[24,55]

(55) Skene, W. G.; Trefz, T. *Polym. Prepr.* **2004**, *45*, 563−564.

Conclusion

The first example of a simple modular route for conjugated thiophene analogues was presented. This self-assembled approach leads to quantitative and selective addition of the thiophenes units that can be controlled by either stoichiometry or solvents and allows for fine-tuneable physical properties of the end products. Through selective unsymmetric and symmetric conjugated compounds, materials with dial-in properties are accessible. Reversible-type oxidation and moderately low

potentials make these azomethines suitable for p-type doping applications, while their linear and planar conformations impart a high degree of conjugation. Such attributes open a new realm of stable thiophene-containing materials with a property of tailoring, and of importance the band-gaps and emissions, which can easily be had unlike their nitrogen-free derivatives. Access to these synthetically simple compounds with varible properties will ultimately yield new materials suitable for functional devices with new operating properties. The inherently weak emission of the thiophene azomethines, low oxidation potential, and reversible radical cation formation potentially make these compounds suitable as PEDOT hole injection replacements in organic light emitting diodes.

Experimental Section

Synthesis. 5-(Thiophen-2-yl)thiophene-2-carbaldehyde (1). In a round-bottom flask was added phosphorus oxychloride (1.83 g, 12 mmol) at 0 °C to DMF (15 mL). After 30 min, 2,2′-bithiophene (500 mg, 3.0 mmol) was added, and the solution was stirred at room temperature for 30 min. The temperature was raised to 50 °C and then held at this temperature until the reaction was completed. Diluted hydrochloric acid was added to the reaction mixture at 0 °C. The crude product was extracted with ethyl acetate after the mixture was warmed to room temperature. Purification by flash chromatography (SiO_2) with 20% ethyl acetate and 80% hexanes yielded the title product as a light brown powder (81%). ^{1}H NMR (400 MHz, acetone-d_6): δ = 9.93 (s, 1H), 7.90 (d, 1H, J = 3.9 Hz), 7.60 (d, 1H, J = 5.2 Hz), 7.52 (d, 1H, J = 4.0 Hz) 7.43 (d, 1H, J = 3.9 Hz), 7.11 (t, 1H, J = 5.2 Hz). ^{13}C NMR (100 MHz, acetone-d_6): δ = 183.2, 146.5, 142.5, 138.5, 136.2, 129.0, 127.9, 126.8, 125.1. HR-MS calcfor $C_9H_7OS_2$ (MH^+), 194.99328; found, 194.99274.

2,5-Diamino-thiophene-3,4-dicarboxylic Acid Diethyl Ester (2). The optimized procedure is based on similar reports.[11,24,25] Sulfur (4.53 g, 0.14 mol) and triethylamine (7.09 mL, 0.05 mol) were stirred in DMF (15 mL) in a 250 mL three-necked flask whereupon the solution turned red within 30 min of stirring at room temperature. Ethyl cyanoacetate (20.4 mL, 0.19 mol) diluted in DMF (5 mL) was subsequently added dropwise over 30 min. The opaque solution was allowed to stir under ambient conditions for 3 days, after which the solvent was removed under vacuum, to yield a brown solid. The solid was loaded onto a silica column and eluted with 100% hexanes gradient up to 35% ethyl acetate. The procedure was repeated a second time to obtain the title compound (2.15 g, 9%) as gold flaky crystals. Mp: 155−156 °C. ^{1}H NMR (400 MHz, acetone-d_6): δ = 6.15 (s, 4H), 4.17 (q, 4H, J = 7.1 Hz), 1.25 (t, 6H, J = 7.1 Hz). ^{13}C NMR (100 MHz, acetone-d_6): δ = 166.7, 151.3, 103.7, 61.0, 15.7. EI-MS: m/z 258.1 ([M]$^+$, 80%), 212 ([M − C_2H_5O]$^+$, 100%), Anal. Calcd for $C_{10}H_{14}O_4N_2S$: C, 46.50; H, 5.46; N, 10.85; O, 24.74; S, 12.41. Found: C, 45.89; H, 5.10; N, 10.47; S, 12.01. HR-MS calcfor $C_{10}H_{14}O_4N_2SNa$ (MNa^+), 281.05665; found, 281.05649.

(*E*)-Diethyl 2-((Thiophen-2-yl)methyleneamino)-5-aminothiophene-3,4-dicarboxylate (3). To **2** (100 mg, 0.39 mmol) was added 2-thiophene carboxaldehyde (43 mg, 0.38 mmol) in ethanol followed by refluxing for 2 h after the addition of a catalytic amount of trifluoroacetic acid (TFA). The solvent was removed, and the product was isolated (126 mg, 94%) as a yellow solid after purification by flash chromatography (SiO_2) with 40% ethyl acetate and 60% hexanes. Mp: 114−116 °C. ^{1}H NMR (400 MHz, acetone-d_6): δ = 8.26 (s, 1H), 7.64 (d, J = 5.2 Hz, 1H), 7.52 (d, J = 4.0 Hz, 1H), 7.48 (bs, 2H), 7.14 (dd, J = 5.2, 4.0 Hz, 1H), 4.33 (q, J = 7.1 Hz, 2H), 4.20 (q, J = 7.1 Hz, 2H), 1.38 (t, J = 7.1 Hz, 3H), 1.26 (t, J = 7.1 Hz, 3H). ^{13}C NMR (100 MHz, acetone-d_6): δ = 165.0, 164.3, 161.1, 161.0, 146.1, 143.2, 132.9, 132.0, 130.5, 128.4, 101.9, 61.0, 60.0, 14.3, 14.1. HR-MS calcfor $C_{15}H_{17}O_4N_2S_2$ (MH^+), 353.06242; found, 353.06251.

(*E*)-Diethyl 2-((5-(Thiophen-2-yl)thiophen-2-yl)methyleneamino)-5-aminothiophene-3,4-dicarboxylate (4). To **2** (30 mg, 0.12 mmol) was added **1** (40 mg, 0.21 mmol) in isopropanol. The solution was then refluxed for 5 h after the addition of a catalytic amount of trifluoroacetic acid (TFA). The solvent was removed, and the product was isolated as a yellow solid (42 mg, 81%) after purification by flash chromatography (SiO_2) with 40% ethyl acetate and 60% hexanes. Mp: 125 °C. ^{1}H NMR (400 MHz, acetone-d_6): δ = 8.20 (s, 1H), 7.50 (d, J = 5.1, 1H), 7.46 (d, J = 3.9 Hz, 1H), 7.40 (d, J = 3.9, 1H), 7.30 (d, J = 3.9 Hz, 1H), 7.12 (dd, J = 5.1, 3.9 Hz, 1H), 4.35 (q, J = 7.1 Hz, 2H), 4.21 (q, J = 7.1 Hz, 2H), 1.40 (t, J = 7.1 Hz, 3H), 1.27 (t, J = 7.1 Hz, 3H). ^{13}C NMR (100 MHz, acetone-d_6): δ = 165.5, 164.1, 161.8, 146.6, 141.6, 141.1, 137.0, 134.3, 132.6, 130.2, 129.6, 127.7, 126.2, 125.8, 101.0, 61.6, 60.4, 15.1, 15.0. EI-MS: m/z 434.9 ([M]$^+$, 96%). HR-MS calcfor $C_{19}H_{19}N_2O_4S_3$ (MH^+), 435.05015; found, 435.05022.

(2*E*,5*E*)-Diethyl 2,5-Bis((thiophen-2-yl)methyleneamino)-thiophene-3,4-dicarboxylate (5). **2** (100 mg, 0.4 mmol) and 2-thiophene carboxaldehyde (198.8 mg, 1.8 mmol) were refluxed in anhydrous isopropanol (10 mL) in a 25 mL flask, during which the solution turned orange and then red in color within 5 h of refluxing under nitrogen with a catalytic amount of TFA. The solution was then concentrated under vacuum to near dryness. The crude product was loaded onto a silica column and eluted with hexanes/ethyl acetate (85%/15% v/v) up to hexanes/ethyl acetate (75%/25% v/v) to give the products as a red solid (65 mg, 36%). Mp: 125−126 °C. ^{1}H NMR (400 MHz, acetone-d_6): δ = 8.75 (s, 2H), 7.85 (d, 2H, J = 5.2), 7.76 (d, 2H, J = 3.7), 7.26 (dd, 2H, J = 5.2, 3.7), 4.31 (q, 4H, J = 7.2), 1.36 (t, 6H, J = 7.2). ^{13}C NMR (100 MHz, acetone-d_6): δ = 163.0, 153.60, 149.2, 142.4, 135.1, 133.2, 128.9, 127.5, 61.2, 14.2. HRMS calcfor $C_{20}H_{19}O_4N_2S_3$ (MH^+), 447.05015; found, 447.04921.

(2*E*,5*E*)-Diethyl 2,5-Bis((5-(thiophen-2-yl)thiophen-2-yl)methyleneamino)thiophene-3,4-dicarboxylate (6). To **2** (49 mg, 0.19 mmol) was added **1** (75 mg, 0.39 mmol), and the solution was then refluxed in isopropanol for 4 h along with a catalytic amount of TFA. The product was isolated as a red powder (58 mg, 50%) after column chromatography (SiO_2), eluted first with 50% ethyl acetate and 50% hexanes, and then with 100% acetone. Mp: 130−132 °C. ^{1}H NMR (400 MHz, acetone-d_6): δ = 8.68 (s, 2H), 7.70 (d, 2H, J = 4.0 Hz), 7.57 (d, 2H, J = 5.2 Hz), 7.49 (d, 2H, J = 3.6 Hz), 7.41 (d, 2H, J = 4.0 Hz), 7.16 (dd, 2H, J = 5.2, 3.6 Hz), 4.34 (q, 4H, J = 6.9 Hz), 1.39 (t, 6H, J = 6.9 Hz). ^{13}C NMR (100 MHz, acetone-d_6): δ = 162.9, 153.8, 149.1, 143.7, 140.2, 137.4, 136.3, 129.4, 128.2, 126.8, 126.7, 125.8, 61.5, 14.6. EI-MS: m/z 610.9 ([M]$^+$, 100%). HR-MS calcfor (MH^+) exact mass, 611.0255; found, 611.0252.

(2*E*,5*E*)-Diethyl 2-((5-(Thiophen-2-yl)thiophen-2-yl)methyleneamino)-5-((thiophen-2-yl)methyleneamino)thiophene-3,4-dicarboxylate (7). This compound was synthesized either in a stepwise manner or by a one-pot approach. Stepwise formation was achieved from **2** (48 mg, 0.19 mmol) to which was added **1** (30

(56) (a) Frère, P.; Raimundo, J.-M.; Blanchard, P.; Delaunay, J.; Richomme, P.; Sauvajol, J.-L.; Orduna, J.; Garin, J.; Roncali, J. *J. Org. Chem.* **2003**, *68*, 7254−7265. (b) Jestin, I.; Frère, P.; Mercier, N.; Levillain, E.; Stievenard, D.; Roncali, J. *J. Am. Chem. Soc.* **1998**, *120*, 8150−8158. (c) Elandaloussi, E. H.; Frère, P.; Richomme, P.; Orduna, J.; Garin, J.; Roncali, J. *J. Am. Chem. Soc.* **1997**, *119*, 10774−10784. (d) Geisler, T.; Petersen, J. C.; Bjornholm, T.; Fischer, E.; Larsen, J.; Dehu, C.; Bredas, J.-L.; Tormos, G. V.; Nugara, P. N. *J. Phys. Chem.* **1994**, *98*, 10102−10111.

(57) (a) Wei, Y.; Chan, C. C.; Tian, J.; Jang, G. W.; Hsueh, K. F. *Chem. Mater.* **1991**, *3*, 888−897. (b) Meerholz, K.; Heinze, J. *Electrochim. Acta* **1996**, *41*, 1839−1854.

(58) (a) Audebert, P.; Catel, J.-M.; Le Coustumer, G.; Duchenet, V.; Hapiot, P. *J. Phys. Chem.* **1995**, *99*, 11923−11929. (b) Facchetti, A.; Yoon, M.-H.; Stern, C. L.; Hutchison, G. R.; Ratner, M. A.; Marks, T. J. *J. Am. Chem. Soc.* **2004**, *126*, 13480−13501. (c) Barbarella, G.; Favaretto, L.; Sotgiu, G.; Zambianchi, M.; Fattori, V.; Cocchi, M.; Cacialli, F.; Gigli, G.; Cingolani, R. *Adv. Mater.* **1999**, *11*, 1375−1379.

mg, 0.15 mmol), and the solution was refluxed with isopropanol for 12 h along with a catalytic amount of TFA. The intermediate product was isolated as a yellow powder (50 mg, 77%) after purification by flash column chromatography (SiO_2) with 40% ethyl acetate and 60% hexanes as solvent. To the isolated product was added 2-thiophene carboxaldehyde (13 mg, 0.12 mmol) in isopropanol in addition to a catalytic amount of TFA. The reaction was refluxed for 12 h. A red colored powder (37.5 mg, 63%) was isolated after flash column chromatography (SiO_2) eluted with hexanes up to hexanes/ethyl acetate (80%/20% v/v). Mp: 128 °C. ^{1}H NMR (400 MHz, acetone-d_6): δ = 8.74 (s, 1H), 8.68 (s, 1H), 7.84 (d, J = 5.2 Hz, 1H), 7.76 (d, J = 3.9 Hz, 1H), 7.70 (d, J = 3.9 Hz, 1H), 7.57 (d, J = 5.2, 1H), 7.50 (d, J = 3.9 Hz, 1H), 7.41 (d, J = 3.9 Hz, 1H), 7.25 (dd, J = 5.2, 3.9 Hz, 1H), 7.16 (dd, J = 5.2, 3.7 Hz, 1H), 4.40−4.25 (m, 4H), 1.45−1.30 (m, 6H). ^{13}C NMR (100 MHz, acetone-d_6): δ = 162.6, 153.1, 152.5, 148.8, 144.4, 144.3, 143.7, 142.1, 140.5, 136.4, 135.8, 134.7, 134.0, 132.8, 128.6, 128.5, 126.9, 125.7, 124.8, 60.8, 60.7, 13.7, 13.6. HR-MS calculated for $C_{24}H_{21}N_2O_4S_4$ (MH^+) exact mass, 529.03787; found, 529.03676.

Alternatively, **2** (100 mg, 0.39 mmol) and 2-thiophene carboxaldehyde (36 mg, 0.32 mmol) were combined in ethanol along with a catalytic amount of TFA. After the mixture was refluxed for 12 h, a yellow powder was isolated after purification by flash chromatography (103 mg, 91%). To the isolated product was added **1** (147 mg, 0.76 mmol) in isopropanol along with a catalytic amount of TFA. A red colored powder (61 mg, 40%) was isolated after flash column chromatography (SiO_2).

One-pot formation of the title compound was achieved by combining **2** (15 mg, 0.06 mmol) with 2-thiophene carboxaldehyde (6.5 mg, 0.06 mmol) followed by refluxing in ethanol for 12 h in the presence of a catalytic amount of TFA. After removal of the solvent, isopropanol was added along with **1** (11.3 mg, 0.06 mmol) and a catalytic amount of TFA. The mixture was then refluxed for 12 h, and the title compound was quantitatively isolated as a red powder after flash chromatography (SiO_2).

The unsymmetric **7** was also prepared stepwise by the addition of **3** (126 mg, 0.4 mmol) to **1** (70 mg, 0.4 mmol) or by the addition of **4** (10 mg, 0.02 mmol) to thiophene carboxaldehyde (3 mg, 0.02 mmol). The general procedure is as follows: The aldehyde was dissolved in anhydrous toluene under nitrogen at 0 °C to which was subsequently added 1,4-diazabicyclo[2.2.2]octane (DABCO) (5 equiv) followed by the slow addition of titanium(IV) chloride ($TiCl_4$) in toluene [1 M] (1 equiv) over 30 min. The reaction was subsequently warmed to room temperature followed by the addition of the corresponding amine, which was dissolved in anhydrous toluene and then refluxed for 1 h. Upon cooling to room temperature, the reaction was filtered through a plug of silica (SiO_2), and the title compound was isolated as a red color powder by C-18 reverse phase preparative HPLC with 70% acetonitrile/30% water as the mobile phase.

3,4-Didecyl-thiophene-2-carbaldehyde. To a solution of 3,4-didecyl-thiophene (188.5 mg, 0.51 mmol) and freshly distilled TMEDA (0.1 mL, 0.66 mmol) in anhydrous hexane (5 mL) under nitrogen was added a solution of *n*-BuLi (2.18 M in hexanes) (0.25 mL, 0.55 mmol) dropwise at room temperature. After the mixture was refluxed for 1 h, THF (3 mL) was added, and the solution was cooled at −78 °C, to which was added DMF (0.1 mL, 1.36 mmol) dropwise. The reaction mixture was hydrolyzed with water (20 mL) after 1.5 h at room temperature, and the mixture was extracted with ethyl acetate. The organic layers were dried over $MgSO_4$ and then concentrated. The crude product was loaded onto a 12+M Biotage column and eluted with hexanes/ethyl acetate up to (98%/2% v/v) over 20 column volumes to afford the product as a colorless oil (61 mg, 30%). ^{1}H NMR (400 MHz, $CDCl_3$): δ = 10.01 (s, 1H), 7.34 (s, 1H), 2.87 (t, 2H, J = 7.6 Hz), 2.53 (t, 2H, J = 7.6 Hz), 1.60 (qt, 2H, J = 5.4 Hz), 1.56 (qt, 2H, J = 5.4 Hz), 1.26 (bs, 28H), 0.88 (t, 6H, J = 5.1 Hz). ^{13}C NMR (100 MHz, $CDCl_3$): δ = 182.7, 151.6, 144.4, 138.2, 130.3, 31.9, 31.9, 29.8, 29.6, 29.6, 29.5, 29.5, 29.4, 29.3, 29.3, 28.3, 27.0, 22.7, 14.1. HR-MS calculated for $C_{25}H_{45}OS$ (MH^+), 393.3185; found, 393.3177.

2,5-Bis-[(thiophen-2-ylmethylene)-amino]-thiophene-3,4-dicarboxylic Acid Diethyl Ester (8). **2** (20 mg, 0.077 mmol) and 3,4-didecyl-thiophene-2-carbaldehyde (60 mg, 0.15 mmol) were refluxed in isopropanol with a catalytic amount of TFA. The mixture was concentrated after refluxing for 4 h. The crude product was loaded onto a silica column and eluted with ether/ethyl acetate (10%/90% v/v) to afford the title compound as a red solid (49 mg, 65%). Mp: 46−48 °C. ^{1}H NMR (400 MHz, acetone-d_6): δ = 8.69 (s, 2H), 7.45 (s, 2H), 4.29 (q, 4H, J = 7.2 Hz), 2.91 (t, 4H, J = 7.6 Hz), 2.60 (t, 4H, J = 7.6 Hz), 1.67 (qt, 4H, J = 7.6 Hz), 1.62 (qt, 4H, J = 7.6 Hz), 1.30 (bs, 62H), 0.88 (t, 6H, J = 7.6 Hz), 0.85 (t, 6H, J = 7.6 Hz). ^{13}C NMR (100 MHz, acetone-d_6): δ = 164.6, 153.6, 151.1, 150.7, 145.9, 138.2, 128.9, 128.3, 62.6, 33.7, 33.7, 33.3, 31.7, 31.4, 30.1, 28.6, 24.3, 15.4. HR-MS calculated for $C_{60}H_{99}O_4N_2S_3$ (MH^+), 1007.6761; found, 1007.6733.

Acknowledgment. We acknowledge financial support from the Natural Sciences and Engineering Research Council Canada, Canada Foundation for Innovation, Fonds de Recherche sur la Nature et les Technologies, and the Centre for Self-Assembled Chemical Structures. Appreciation is extended to Dr. M. Simard for assistance with the crystal structure analysis and to Prof. D. Zargarian for helpful suggestions. M.B. thanks the Université de Montréal for a graduate scholarship.

Supporting Information Available: General experimental procedure, reagents, and materials. ^{1}H and ^{13}C NMR spectra of compounds **1**−**7**, absorption, fluorescence, and phosphorescence spectra of compounds **2**−**7**, and uncorrected cyclic voltammograms of compounds **3**−**7**. Details of the crystal structure determination of **7**. This material is available free of charge via the Internet at http://pubs.acs.org.

JO070100O